1732 *Organometallics* 1984, *3*, 1732–1739

Binuclear Metal Carbonyl R-DAB Complexes.[1] Conversion of Coordinated 1,4-Diaza-1,3-butadienes into 3-Amino-1-azaallyl Monoanions by Interaction with $[HFe(CO)_4]^-$. Molecular Structure of $[FeMn(CO)_6\{(t\text{-Bu})N\cdots CH\cdots CHN(H)(t\text{-Bu})\}]$, Containing an η^3-1-Azaallyl Moiety Bonded to Fe

Jan Keijsper,[†] John Mul,[†] Gerard van Koten,[†] Kees Vrieze,*[†] Henk C. Ubbels,[‡] and Casper H. Stam[‡]

Laboratorium voor Anorganische Chemie and Laboratorium voor Kristallografie, University of Amsterdam, 1018 WV Amsterdam, The Netherlands

Received September 21, 1983

The reaction of $[HFe(CO)_4]^-$ with $[M(CO)_3(\text{R-DAB}\{R_1,R_2\})Br]$ (R-DAB$\{R_1,R_2\}$ = 1,4-disubstituted 1,4-diaza-1,3-butadiene = $RN{=}C(R_1)C(R_2){=}NR$, M = Mn, $R_1 = R_2$ = H, R = c-Hex, *t*-Bu, *p*-tol; M = Mn, $R_1 = R_2 = CH_3$, R = c-Pr; M = Mn, R_1 = H, $R_2 = CH_3$, R = *i*-Pr; M = Re, $R_1 = R_2$ = H, R = *i*-Pr, *t*-Bu) at 40 °C in THF solution yields the novel heterodinuclear species $[FeMn(CO)_6(\text{R-AAA}\{R_1,R_2\})]$ (R-AAA$\{R_1,R_2\}$ = 3-R-amino-1-R-azaallyl = $RN\cdots C(R_1)\cdots C(R_2)N(H)R$).[2] During this reaction, neutral four-electron, σ-N, σ-N′-bonded R-DAB is converted to an eight-electron-bonded, monoanionic 3-R-amino-1-R-azaallyl moiety. The amino substituent containing a new N–H bond coordinates to Mn, while the monoanionic 1-azaallylic moiety is four-electron, η^3-bonded to Fe and two-electron, σ-N-bonded to Mn. This is evidenced by an X-ray crystal structure determination of $[FeMn(CO)_6(t\text{-Bu-AAA})]$. Crystals of $C_{16}H_{21}FeMnN_2O_6$ are monoclinic of space group $P2_1/c$ with cell constants a = 16.044 (1) Å, *b* = 18.220 (2) Å, *c* = 17.330 (2) Å, β = 129.69 (1)°, and *Z* = 8.[4a] A total of 1287 reflections have been used in the refinement, which results in a final *R* value of 0.042. In the asymmetric unit there are two independent molecules having only slightly different geometries. The Fe–Mn distances of 2.616 (5) and 2.640 (4) Å for molecules A and B, respectively, are indicative of a Fe–Mn single bond. The bond lengths within the 3-amino-1-azaallylic $N(1)\cdots C(7)\cdots (C8)N(2)(H)$ moiety are N(1)–C(7) = 1.38 Å (mean), C(7)–C(8) = 1.39 Å (mean), and C(8)–N(2) = 1.45 Å (mean), respectively. Formally, the ligand can be described as an eight-electron donor, being σ-N, σ-N′-coordinated to Mn, with bond lengths Mn–N(1) = 2.02 (mean) and Mn–N(2) = 2.12 (mean) Å, and being η^3-coordinated to Fe (Fe–C(7) = 2.01 Å (mean), Fe–C(8) = 2.08 Å (mean), and Fe–N(1) = 2.04 (mean)). The metal carbonyl skeleton of the complex consists of five terminal carbonyls with normal M–C(carbonyl) bond lengths and M–C–O bond angles and one semibridging CO group: Fe–C(4) = 1.701 (16) and 1.742 (15) Å for molecules A and B, respectively, with corresponding Mn–C(4) distances of 2.627 (12) and 2.547 (11) Å. The Fe–C(4)–O(4) bond angles are 169.3 (14) and 165.3 (12)° for molecules A and B, respectively. Reaction of $[Mn(CO)_3(\text{R-DAB})Br]$ (R = *i*-Pr, *t*-Bu) with $[DFe(CO)_4]^-$ leads to the formation of $[FeMn(CO)_6[RNC(H)C(H)N(D)R)]$ only, which proves that the transferred deuteride (hydride) orginates from the Fe anion reagent. A possible reaction mechanism for the formation of the heterodinuclear R-AAA species is discussed. All complexes have further been characterized by ^1H NMR, ^{13}C NMR, IR, and mass spectroscopy.

Introduction

During our study of the coordination of 1,4-disubstituted 1,4-diaza-1,3-butadienes, R-DAB = $RN{=}CHCH{=}NR$,[2] it was discovered that strong activation of the diimine skeleton can be achieved by coordination of at least one C=N double bond to a metal carbonyl center. Such η^2-C=N coordination, which can be expected when R-DAB is bonded to two metals[3,4b] (see Figure 1), may result in C–C bond formation between the activated R-DAB and various substrates. For example, $Ru_2(CO)_5(\text{R-DAB})$, in which R-DAB is eight-electron bonded, reacts easily with R-DAB to yield $Ru_2(CO)_5(\text{R-IAE})$ (R-IAE = bis[(R-imino)(R-amino)ethane], $RN{=}CHCH(NR)CH(NR)CH{=}NR$).[5] $Ru_2(CO)_6(\text{R-DAB})$, containing a six-electron-coordinated diimine, reacts with various ligands L, such as carbodiimides and sulfines, to give complexes of general formula $Ru_2(CO)_5(\text{R-DAB-L})$, in which R-DAB and L are coupled via a C–C bond.[6] $Ru_2(CO)_6(\text{R-DAB})$ also reacts with acetylenes, giving C–C coupled products, which are excellent precursors for the regiospecific cyclotrimerization of acetylenes.[7]

Because coordination of R-DAB to different metals may present new possibilities for activation of the R-DAB species, we have also attempted to synthesize heterodinuclear R-DAB species. There is considerable interest in the synthesis and reactivity of such heterometallic complexes because of their potential role in heterogeneous as well as homogeneous catalysis.[8] One of the cleanest

---

[†] Laboratorium voor Anorganische Chemie.
[‡] Laboratorium voor Kristallografie.

(1) Part 11: for earlier parts see, e.g., ref 4b, 5, 7, 10, 11, and 30.

(2) (a) The nomenclature for the ligand was developed earlier.[3] R-DAB stands for $RN{=}C(H)C(H){=}NR$, while $RN{=}C(R_1)C(R_2){=}NR$ is abbreviated as R-DAB$\{R_1,R_2\}$. (b) In line with this, for the $RN\cdots C(H)\cdots C(H)N(H)R$ ligand R-AAA is used, while $RN\cdots C(R_1)\cdots C(R_2)N(H)R$ is abbreviated as R-AAA$\{R_1,R_2\}$.

(3) van Koten, G.; Vrieze, K. *Adv. Organomet. Cem.* **1982**, *21*, 151.

(4) (a) Conventional cell: *a* = 16.044 (1) Å, *b* = 18.220 (2) Å, *c* = 14.234 (2) Å, β = 110.46 (1)°, space group $P2_1/n$. (b) Staal, L. H.; Polm, L. H.; Balk, R. W.; van Koten, G.; Vrieze, K.; Brouwers, A. M. F. *Inorg. Chem.* **1980**, *19*, 3343.

(5) Keijsper, J.; Polm, L. H.; van Koten, G.; Vrieze, K.; Abbel, G.; Stam, C. H. *Inorg. Chem.* **1984**, *23*, 2142.

(6) Keijsper, J.; van Koten, G.; Vrieze, K., to be submitted for publication.

(7) Staal, L. H.; van Koten, G.; Vrieze, K.; van Santen, B.; Stam, C. H. *Inorg. Chem.* **1981**, *20*, 3598.

(8) See, e.g.: Gladfelter, W. L.; Geoffroy, G. L. *Adv. Organomet. Chem.* **1980**, *18*, 207 and references therein.

0276-7333/84/2303-1732$01.50/0

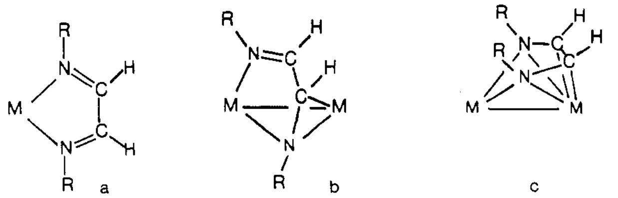

Figure 1. The relevant coordination modes for R-DAB: a, four-electron, σ-N,σ-N'; b, six-electron, σ-N,μ-N', η^2-C=N'; c, eight-electron, σ-N,σ-N', η^2-C=N,η^2-C'=N'.

methods to form (hetero)metal–metal bonds is by interaction of carbonyl metalates with metal halides.[9] Examples demonstrating this approach in ourr R-DAB chemistry are as follows: (i) reaction of $[Mn(CO)_5]^-$ with $[M(CO)_3$(R-DAB)Br] (M = Mn, Re), yielding $(CO)_5MnM(CO)_3$(R-DAB), containing still a four-electron-coordinated R-DAB;[10] (ii) reaction of $[Co(CO)_4]^-$ with $[M(CO)_3$(R-DAB)Br], yielding unstable $[(CO)_4CoM(CO)_3$(R-DAB)] [this substitution reaction is then followed by CO elimination with concomitant formation of an η^2-C=N to Co bond, leading to $[CoM(CO)_6$(R-DAB)], containing a six-electron-coordinated R-DAB];[11] (iii) reaction of $[(\eta^5$-$C_5H_5)Fe(CO)_2]^-$ with $[Mn(CO)_3$(*t*-Bu-DAB)Br], yielding $[Mn_2(CO)_6$(*t*-Bu-DAB)],[12] containing an eight-electron-bonded R-DAB as has been established for $[Mn(CO)_6$-(Me-DAB{Me,Me})].[13] In all these examples R-DAB remains neutral with its diimine skeleton planar and intact. We now, however, report the reaction of $[HFe(CO)_4]^-$ with $[M(CO)_3$(R-DAB)Br] (M = Mn, Re), which results not only in the formation of a heterometal–metal bond but also in the conversion of the R-DAB ligand to an anionic ligand by partial reduction of one double bond.

Experimental Section

Materials and Apparatus. ^1H NMR spectra were obtained on a Varian T60 or a Bruker WM250 spectrometer; ^{13}C NMR spectra have been recorded with a Bruker WP80 spectrometer. IR spectra were obtained on a Perkin-Elmer 283 spectrometer and mass spectra on a Varian MAT 711 mass spectrometer, applying field desorption techniques. Elemental analyses were obtained from the elemental analyses section of the Institute for Applied Chemistry, TNO, Utrecht, The Netherlands.

The R-DAB$\{R_1,R_2\}$ ligands[14] and $[M(CO)_3$(R-DAB$\{R_1,R_2\}$)Br] (M = Mn, Re)[15] have been prepared according to the literature procedures.

Synthesis of $[FeMn(CO)_6$(R-AAA$\{R_1,R_2\}$)].[2] A THF solution of $Na[HFe(CO)_4]$ was prepared according to a modified literature procedure, described below.[16] In a typical experiment 1.0 g of NaOH (25 mmol) was dissolved in 3 mL of H_2O and 3.5 mL of MeOH was added. N_2 was bubbled through this solution for 0.5 h, and then 0.7 mL of $Fe(CO)_5$ (5.2 mmol) was added by syringe. After 30 min unreacted MeOH, H_2O, and $Fe(CO)_5$ were evaporated in vacuo and the remaining $Na[HFe(CO)_4]$ was extracted with 4 × 20 mL of THF and dried with Na_2SO_4. The solution was slightly red due to the presence of some anionic polyiron hydride species, but IR spectra of the terminal ν(CO) region showed the ν(CO) vibrations of $[HFe(CO)_4]^-$ only: 1996 (m), 1905 (sh), and 1876 (vs) cm^{-1}. To this solution was added 3 mmol of $[M$-$(CO)_3$(R-DAB$\{R_1,R_2\}$)Br] and then the mixture stirred for 16 h at 40 °C. The resulting mixture was filtered and the filtrate concentrated, leaving a residue that was purified by column chromatography (silica; eluant hexane/ether; 1/1). Crystallization at −80 °C yielded orange/red (M = Mn; 70% yield based on Mn) or yellow (M = Re; 50% yield based on Re) crystals that were identified as $[FeM(CO)_6$(R-AAA$\{R_1,R_2\}$)] by elemental analysis, IR, ^1H NMR, ^{13}C NMR, and FD-mass spectrometry (see Tables IV–VI), and an X-ray structure determination of $[FeMn(CO)_6$-(*t*-Bu-AAA)]. $[FeMn(CO)_6$(*p*-tol-AAA)] could only be obtained in yields lower than 5%. For the compounds with M = Re and R = *i*-Pr as well as M = Mn and R = *p*-tol, elution of the reaction mixtures with hexane yielded a yellowish fraction containing a hydride product, which is isomeric with the 3-amino-1-azaallylic derivative and was identified as $[HFeM(CO)_6$(R-DAB)].[17]

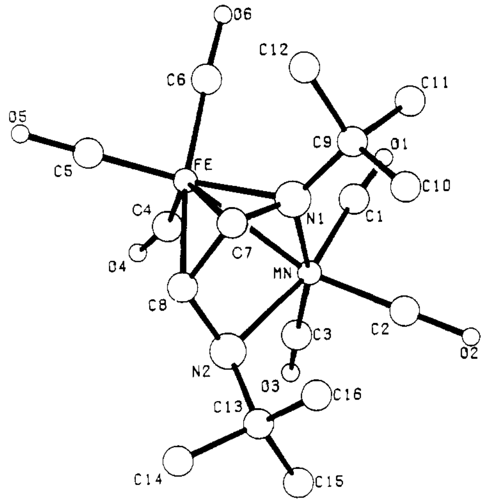

Figure 2. The molecular geometry of $[FeMn(CO)_6$(*t*-Bu-AAA)] (molecule A).

A THF solution of $Na[DFe(CO)_4]$ was prepared analogously to that of $Na[HFe(CO)_4]$ by using $NaOD/D_2O$ and methanol-d_4. Reactions with $[Mn(CO)_3$(R-DAB)Br] (R = *t*-Bu, *i*-Pr) involved the same procedure as described above.

Crystal Structure Determination of $[FeMn(CO)_6$(*t*-Bu-AAA)] ($C_{16}H_{21}FeMnN_2O_6$; Hexacarbonyl[3-(*tert*-butylamino)-1-*tert*-butyl-1-azaallyl]ironmanganese). Crystals of the title compound were of rather poor quality, but nevertheless one of sufficient quality was selected for a crystal structure determination. The crystals were monoclinic of space group $P2_1/c$. The unit cell had the following dimensions: a = 16.044 (1) Å, b = 18.220 (2) Å, c = 17.330 (2) Å, β = 129.69 (1)°;[4a] Z = 8; V = 3898.3 (5) Å^3; d_{calcd} = 1.52 g cm^{-3}. A total of 1334 independent reflections of which 1287 ($-10 \le h \le 11$, $0 \le k \le 13$, $-10 \le l \le 12$) had intensities above the $2.5\sigma(I)$ level were measured on a Nonius CAD 4 diffractometer using graphite-monochromated Cu Kα radiation ($\theta < 35°$). An absorption correction was applied (crystal dimensions 0.04 × 0.15 × 0.16 mm; μ = 116.2 cm^{-1}; minimum and maximum corrections 1.53 and 5.30, respectively). The positions of the four metal atoms in the asymmetric unit were

---

[9] Chisholm, M. H.; Rothwell, I. P. *Prog. Inorg. Chem.* **1982**, *29*, 1.

[10] Staal, L. H.; van Koten, G.; Vrieze, K. *J. Organomet. Chem.* **1979**, *175*, 73.

[11] Staal, L. H.; Keijsper, J.; van Koten, G.; Vrieze, K.; Cras, J. A.; Bosman, W. P. *Inorg. Chem.* **1981**, *20*, 555.

[12] Keijsper, J.; van Koten, G.; Vrieze, K., to be submitted for publication.

[13] Adams, R. D. *J. Am. Chem. Soc.* **1980**, *102*, 7476.

[14] (a) Kliegman, J. M.; Barnes, R. K. *J. Org. Chem.* **1970**, *35*, 3140. (b) Staal, L. H.; Polm, L. H.; Vrieze, K.; Ploeger, F.; Stam, C. H. *Inorg. Chem.* **1981**, *20*, 3590.

[15] Staal, L. H.; Oskam, A.; Vrieze, K. *J. Organomet. Chem.* **1979**, *170*, 235.

[16] Darensbourg, M. Y.; Darensbourg, D. J.; Barros, H. C. *Inorg. Chem.* **1978**, *17*, 297.

[17] (a) When, e.g., $[Re(CO)_3$(*i*-PR-DAB)Br] is reacted with $[HFe(CO)_4]^-$, two isomeric products are formed. Fraction A (eluant hexane): $[HFeRe(CO)_6$(*i*-Pr-DAB)]; IR (ν(CO), hexane solution) 2061 (m), 2013 (s), 1995 (s), 1920 (vs) cm^{-1}; ^1H NMR ($CDCl_3$ solution) δ −16.48 (1 H, s), 1.09 (3 H, d, J = 6 Hz), 1.21 (3 H, d, J = 6 Hz), 1.43 (3 H, d, J = 6 Hz), 1.56 (3 H, d, J = 6 Hz), 2.28 (1 H, septet, J = 6 Hz), 3.49 (1 H, septet, J = 6 Hz), 4.01 (1 H, d, J = 2 Hz), 8.03 (1 H, d, J = 2 Hz). According to these data,[28] the diimine ligand is in a six-electron-coordination mode. A crystal structure determination of analogous $[HFeMn(CO)_6\{C_5H_4N$-2-CH=N-(*t*-Bu)$\}]$ showed that the hydride is asymmetrically bridging the two metals. Fraction B (eluant hexane/ether, 1/1): $[FeRe(CO)_6$(*i*-Pr-AAA)]. When this compound is heated in toluene, it reacts via a first-order reaction path to yield the isomeric hydride $[HFeRe(CO)_6$(*i*-Pr-DAB)]. Full details will be given in a forthcoming paper. (b) For M = Mn and R = *p*-tol, the major product of the reaction of $[Mn(CO)_3$(*p*-tol-DAB)Br] with excess $[HFe(CO)_4]^-$ is $[HFeMn(CO)_6\{N$(*p*-tol)CH_2CH_2N(*p*-tol)$\}]$ for which crystal structure and spectral properties will be published shortly.

Table I. The Atomic Coordinates of $[\mathrm{FeMn(CO)_6\{(\mathit{t}\text{-}Bu)NC(H)C(H)N(H)(\mathit{t}\text{-}Bu)\}}]$

	molecule A			molecule B		
	x	*y*	*z*	*x*	*y*	*z*
Mn	0.6506 (2)	0.3068 (2)	0.1787 (2)	0.8817 (2)	0.6666 (1)	0.6934 (2)
Fe	0.5026 (2)	0.3929 (1)	0.1502 (2)	0.7310 (2)	0.5724 (2)	0.6476 (2)
C(1)	0.6841 (11)	0.3669 (7)	0.1222 (10)	0.9158 (10)	0.6248 (8)	0.6251 (9)
C(2)	0.7851 (10)	0.2711 (8)	0.2579 (10)	1.0150 (11)	0.6986 (8)	0.7838 (10)
C(3)	0.6105 (11)	0.2472 (8)	0.0828 (10)	0.8496 (11)	0.7419 (8)	0.6160 (11)
C(4)	0.4474 (10)	0.3465 (8)	0.0420 (10)	0.6874 (10)	0.6299 (8)	0.5478 (9)
C(5)	0.3848 (11)	0.4224 (8)	0.1298 (11)	0.6066 (11)	0.5516 (8)	0.6165 (10)
C(6)	0.5194 (10)	0.4789 (7)	0.1171 (10)	0.7304 (10)	0.4890 (8)	0.5989 (10)
C(7)	0.5930 (9)	0.3595 (7)	0.2938 (9)	0.8279 (10)	0.5869 (7)	0.7959 (9)
C(8)	0.5255 (9)	0.3023 (7)	0.2346 (9)	0.7577 (9)	0.6471 (7)	0.7499 (9)
C(9)	0.7453 (10)	0.4356 (8)	0.3450 (10)	0.9755 (10)	0.5177 (7)	0.8254 (9)
C(10)	0.8338 (10)	0.3970 (8)	0.4453 (10)	1.0684 (11)	0.5485 (8)	0.9299 (10)
C(11)	0.8003 (11)	0.4646 (8)	0.3042 (11)	1.0196 (11)	0.4995 (8)	0.7721 (11)
C(12)	0.6994 (11)	0.5015 (8)	0.3616 (11)	0.9311 (12)	0.4468 (8)	0.8361 (10)
C(13)	0.6208 (10)	0.1794 (7)	0.2929 (9)	0.8454 (10)	0.7696 (8)	0.8258 (10)
C(14)	0.5348 (10)	0.1489 (8)	0.2976 (10)	0.7548 (11)	0.7930 (8)	0.8282 (12)
C(15)	0.6507 (12)	0.1220 (8)	0.2518 (11)	0.8860 (12)	0.8363 (8)	0.8034 (11)
C(16)	0.7155 (11)	0.2069 (7)	0.3943 (10)	0.9397 (11)	0.7355 (8)	0.9263 (10)
N(1)	0.6608 (7)	0.3780 (5)	0.2743 (7)	0.8922 (7)	0.5785 (5)	0.7691 (7)
N(2)	0.5696 (8)	0.2428 (5)	0.2157 (7)	0.8026 (8)	0.7139 (6)	0.7419 (7)
O(1)	0.7068 (8)	0.4028 (6)	0.0825 (7)	0.9341 (7)	0.6001 (5)	0.5750 (6)
O(2)	0.8712 (7)	0.2486 (6)	0.3097 (7)	1.1023 (7)	0.7220 (6)	0.8413 (7)
O(3)	0.5827 (9)	0.2084 (6)	0.0148 (8)	0.8304 (8)	0.7940 (6)	0.5661 (8)
O(4)	0.3928 (7)	0.3188 (5)	−0.0399 (7)	0.6380 (7)	0.6594 (5)	0.4698 (7)
O(5)	0.3089 (7)	0.4409 (6)	0.1166 (8)	0.5263 (8)	0.5397 (6)	0.6013 (8)
O(6)	0.5302 (7)	0.5358 (5)	0.0932 (7)	0.7291 (8)	0.4315 (5)	0.5678 (7)

derived from an E^2 Patterson synthesis. A subsequent F_o synthesis revealed the remaining non-hydrogen atoms. Refinement was carried out by means of anisotropic block-diagonal least-squares calculations in which the hydrogen atoms, which were indicated in a ΔF synthesis, were included at calculated positions with fixed parameters. The final R value was 0.042, unit weights were applied, and the anomalous dispersion of Fe and Mn was taken into account.[18a] The computer programs used for plotting[18b] the scattering factors and dispersion correction[18a] were taken from the literature.

The molecular geometry of $[\mathrm{FeMn(CO)_6}(t\text{-Bu-AAA})]$ with the numbering of the atoms is given in Figure 2, which shows a PLUTO[18b] drawing of molecule A. Atomic parameters, bond lengths, and selected bond angles are given in Tables I, II, and III, respectively. All bond lengths and angles, anisotropic thermal parameters, and a list of observed and calculated structure factors are included with the supplementary material.

Analytical Data. All complexes gave satisfactory results (Table VII). The complexes showed characteristic ν(CO) and ν(N–H) IR absorptions that are listed in Table IV. Mass spectra have been obtained by using the field desorption technique. Observed and calculated m/z values are also listed in Table IV.

Results

Molecular Structure. In the asymmetric unit there are two independent molecules A and B, which have only slightly different geometries. The molecular geometry of $[\mathrm{FeMn(CO)_6}(t\text{-Bu-AAA})]$ (molecule A) is shown in Figure 2, together with the atomic numbering.

The metal carbonyl part of this heterodinuclear complex consists of a $\mathrm{(CO)_3FeMn(CO)_3}$ unit with a rather short metal–metal bond (2.616 (5) and 2.640 (4) Å for molecules A and B, respectively). This may be compared with other values for Mn–Fe single bonds in dinuclear species ranging from 2.848 (4) to 2.618 (1) Å.[19] Only in a trinuclear $\mathrm{Fe_2Mn}$ compound has a shorter value of 2.561 (1) Å been found.[20]

Table II. Bond Lengths (Å) of $\mathrm{FeMn(CO)_6}(t\text{-Bu-AAA})$ (Esd)

	A	B
	Metal Carbonyl Part	
Fe–Mn	2.616 (5)	2.640 (4)
Fe–C(4)	1.701 (16)	1.742 (15)
Fe–C(5)	1.770 (20)	1.745 (19)
Fe–C(6)	1.748 (15)	1.735 (17)
Mn–C(1)	1.766 (20)	1.763 (20)
Mn–C(2)	1.783 (13)	1.758 (13)
Mn–C(3)	1.729 (17)	1.751 (16)
Mn–C(4)	2.627 (12)	2.547 (11)
C(1)–O(1)	1.164 (24)	1.170 (23)
C(2)–O(2)	1.139 (15)	1.164 (15)
C(3)–O(3)	1.190 (21)	1.185 (20)
C(4)–O(4)	1.204 (17)	1.173 (16)
C(5)–O(5)	1.137 (23)	1.159 (24)
C(6)–O(6)	1.170 (18)	1.172 (19)
	Ligand Part	
N(1)–C(7)	1.371 (23)	1.384 (25)
C(7)–C(8)	1.376 (16)	1.400 (17)
C(8)–N(2)	1.442 (20)	1.465 (19)
N(1)–C(9)	1.523 (15)	1.517 (15)
N(2)–C(13)	1.548 (16)	1.530 (19)
C(9)–C(10)	1.543 (17)	1.539 (16)
C(9)–C(11)	1.535 (31)	1.516 (31)
C(9)–C(12)	1.529 (25)	1.543 (23)
C(13)–C(14)	1.537 (27)	1.541 (29)
C(13)–C(15)	1.506 (27)	1.541 (26)
C(13)–C(16)	1.496 (15)	1.531 (16)
	Metal Ligand Part	
Mn–N(1)	2.027 (13)	2.011 (11)
Mn–N(2)	2.127 (15)	2.103 (16)
Fe–C(7)	2.014 (13)	1.997 (13)
Fe–C(8)	2.077 (15)	2.052 (16)
Fe–N(1)	2.042 (8)	2.044 (8)

Five carbonyls are terminally bound, three to Mn (Mn–C = 1.76 Å (mean); Mn–C–O = 177.3° (mean)) and two to

---

[18] (a) "International Tables for Crystallography"; Kynoch Press: Birmingham, England, 1974; Vol. IV. (b) Motherwell, S.; Clegg, G. "PLUTO", A program for plotting molecular and crystal structures; University of Cambridge: England, 1978.

[19] Gadol, S. M.; Davis, R. E. *Organometallics* **1982**, *1*, 1607.

[20] Kolobova, N. E.; Ivanov, L. L.; Zhvanko, O. S.; Batsanov, A. S.; Struchkov, Y. T. *J. Organomet. Chem.* **1982**, *231*, 37.

Table III. Some Important Bond Angles (deg) of $FeMn(CO)_6(t\text{-}Bu\text{-}AAA)$ (Esd)

	A	B
Metal Carbonyl Part		
Mn-C(1)-O(1)	175.9 (15)	175.9 (11)
Mn-C(2)-O(2)	179.0 (17)	177.4 (14)
Mn-C(3)-O(3)	177.5 (15)	178.0 (11)
Mn-C(4)-O(4)	119.8 (12)	121.3 (12)
Fe-C(4)-O(4)	169.3 (14)	165.3 (12)
Fe-C(5)-O(5)	179.6 (13)	175.8 (15)
Fe-C(6)-O(6)	178.6 (16)	177.7 (18)
Mn-C(4)-Fe	70.7 (4)	73.3 (3)
Around Mn		
Fe-Mn-C(1)	94.8 (6)	97.7 (5)
Fe-Mn-C(2)	150.5 (6)	147.5 (6)
Fe-Mn-C(3)	117.3 (5)	121.0 (5)
Fe-Mn-C(4)	37.9 (4)	39.2 (4)
Fe-Mn-N(1)	50.2 (2)	49.9 (2)
Fe-Mn-N(2)	74.3 (3)	73.5 (3)
C(1)-Mn-C(2)	90.3 (8)	91.1 (8)
C(1)-Mn-C(3)	85.1 (8)	83.7 (9)
C(2)-Mn-C(3)	92.0 (7)	91.0 (7)
C(1)-Mn-N(1)	99.3 (6)	99.2 (6)
C(1)-Mn-N(2)	165.5 (5)	166.1 (4)
C(2)-Mn-N(1)	100.2 (6)	97.8 (6)
C(2)-Mn-N(2)	103.9 (7)	102.1 (7)
C(3)-Mn-N(1)	166.9 (6)	170.6 (6)
C(3)-Mn-N(2)	91.2 (7)	91.6 (8)
N(1)-Mn-N(2)	81.4 (5)	83.5 (5)
Around Fe		
Mn-Fe-C(4)	71.4 (5)	67.5 (47)
Mn-Fe-C(5)	160.8 (5)	151.8 (5)
Mn-Fe-C(6)	106.7 (6)	115.8 (6)
Mn-Fe-C(8)	70.1 (5)	70.3 (5)
N(1)-Fe-C(4)	121.1 (6)	115.6 (6)
N(1)-Fe-C(5)	134.5 (7)	140.8 (7)
N(1)-Fe-C(6)	96.7 (15)	99.1 (5)
N(1)-Fe-C(8)	67.1 (4)	69.2 (5)
C(4)-Fe-C(5)	101.1 (7)	99.7 (7)
C(4)-Fe-C(6)	99.5 (8)	99.8 (8)
C(4)-Fe-C(8)	96.6 (7)	100.9 (6)
C(5)-Fe-C(6)	91.8 (8)	90.6 (8)
C(5)-Fe-C(8)	93.9 (7)	88.7 (7)
C(6)-Fe-C(8)	161.6 (5)	159.1 (6)
Ligand Part		
Mn-N(1)-Fe	80.0 (3)	81.2 (3)
Mn-N(1)-C(7)	112.4 (7)	111.2 (8)
Mn-N(1)-C(9)	131.6 (12)	132.5 (11)
Fe-N(1)-C(7)	69.2 (6)	68.1 (6)
Fe-N(1)-C(9)	128.7 (7)	129.7 (7)
Mn-N(2)-C(8)	98.0 (8)	99.0 (9)
Mn-N(2)-C(13)	125.5 (9)	129.2 (10)
Fe-C(8)-N(2)	109.2 (12)	108.3 (12)
C(7)-N(1)-C(9)	114.2 (13)	113.9 (12)
N(1)-C(7)-C(8)	111.9 (15)	113.4 (14)
C(8)-N(2)-C(13)	115.6 (13)	114.2 (13)
N(2)-C(8)-C(7)	118.2 (13)	116.1 (13)

Fe (Fe–C = 1.75 Å (mean); Fe–C–O = 177.9° (mean)). The bridging carbonyl C(4)O(4) is in one plane with the two metals. The large difference in the M–C(4) bond lengths (Fe–C(4) = 1.72 Å (mean); Mn–C(4) = 2.59 Å (mean)) as well as the large difference in bond angles (Fe–C(4)–O(4) = 167.3° (mean); Mn–C(4)–O(4) = 120.6° (mean)) justify the classification of this carbonyl group as a semibridging one.[21] This type of bridging mode for carbonyls is considered as an intermediate stage between bridging and terminal coordination in CO exchange processes on metal clusters. The are often present to finely counterbalance electronic effects between two metals that may variously arise from the presence of two different metals, another asymmetrically bridging ligand, or a donative metal–metal bond.[22a] Curtis et al. have reported a correlation between the observed asymmetry α[22b] in the CO bridge and the carbonyl bond angle for a series of complexes containing a semibridging or an asymmetrically bridging CO group.[23] The corresponding values found for the present structure fit perfectly into the extreme part of the correlation plot, indicating that the present semibridging C(4)O(4) carbonyl group may be considered as a nearly terminal one.

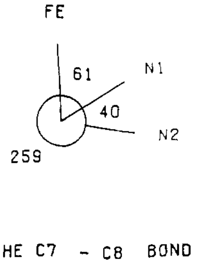

Figure 3. The Newman projection along C(7)–C(8), showing the asymmetry in the ligand.

The bond lengths and distances within the metal–t-Bu-AAA part of the molecule point to a four-electron, σ-N,σ-N′-type of coordination of the ligand toward Mn and to a four-electron, η^3-azaallylic one toward Fe. Accordingly, the ligand is bonded to Mn via N(1) and N(2) with different bond lengths of 2.02 (mean) and 2.12 A (mean), respectively. The difference may be due to the differing hybridization of these nitrogen atoms, being sp² and sp³, respectively. The azaallylic part is η^3-bonded to Fe with similar bond lengths: Fe–N(1) = 2.04 Å (mean), Fe–C(7) = 2.01 Å (mean), and Fe–C(8) = 2.06Å (mean). In the only other structurally characterized iron 1-azaallyliuc complex, i.e., $[Fe_2(CO)_6\{(C_{10}H_{11})N{=}C(CO_2Me)\overset{\cdots}{-}C(CO_2Me)\}]$, comparable values of 1.99, 1.99, and 2.19 Å, respectively, have been found.[24]

The intraligand bond lengths are also in line with an η^3-azaallylic bond description. The N(1)–C(7) and C(7)–C(8) bond lengths within the η^3-bonded part of the ligand are equal (1.38 Å) and distinctly longer than the formally single N(2)–C(8) bond length (1.45 Å). Similar features are observed in $[Ru_2(CO)_5\{(i\text{-}Pr)N\overset{\cdots}{-}CH\overset{\cdots}{-}CHN(i\text{-}Pr)C(O)CH_2C(O)CH_2\}]$,[25] containing equal intraazaallylic distances of 1.40 Å with a N–C single bond length of 1.46 Å, and in $[Fe_2(CO)_6\{(C_{10}H_{11})N\overset{\cdots}{-}C(CO_2Me)\overset{\cdots}{-}C(CO_2Me)\}]$, containing equal intraazaallylic bond lengths of 1.42 Å.

The η^3-bonded ligand in $[(\eta^5\text{-}C_5H_5)Mo(I)(CO)\{C(NMe_2)C(Me)N(Me)\}]$ is described as a carbene with an adjacent η^2-C=N bond to Mo.[26] This different bonding situation is apparent from the different intraligand C–C and N–C bond lengths of 1.33 and 1.46 Å, respectively, as well as from the observation that one short Mo–C(carbene) is present together with two long Mo–N and Mo–C distances.

In [FeMn(CO)$_6$(t-Bu-AAA)] the torsion angle between the two C–N bonds of the ligand's skeleton shows that the

---

[21] Colton, R.; McCormick, M. J. *Coord. Chem. Rev.* **1980**, *31*, 1.

[22] (a) Cotton, F. A.; Kruczynski, L.; Frenz, B. A. J. *J. Organomet. Chem.* **1978**, *160*, 93 and references therein. (b) The α value of 0.5 for [FeMn(CO)$_6$(t-Bu-AAA)] falls near the weak interaction end of the semibridging region. Compare: Curtis, M. D.; Han, K. R.; Butler, W. M. *Inorg. Chem.* **1980**, *19*, 2096.

[23] Klingler, B. J.; Butler, W. M.; Curtis, D. M. *J. Am. Chem. Soc.* **1978**, *100*, 5034.

[24] Nakamura, J.; Bachmann, K.; Heimgarten, H.; Schmidt, H.; Daly, J. J. *Helv. Chim. Acta* **1978**, *61*, 589.

[25] Polm, L. H.; van Koten, G.; Vrieze, K.; Stam, C. H.; van Tunen, W. C. J. *J. Chem. Soc., Chem. Commun.* **1983**, 1177.

[26] Adams, R. D.; Chodosk, D. F. *J. Am. Chem. Soc.* **1977**, *99*, 6544.

[27] Staal, L. H.; van Koten, G.; Fokkens, R. H.; Nibbering, N. M. M. *Inorg. Chim. Acta* **1981**, *50*, 205.

Table IV. FD-Mass and IR Data for [FeM(CO)$_6$(RN⋯C(R$_1$)⋯C(R^2)N(H)R)]

compd	M obsd[a] (calcd)	ν(NH)[b]	ν(CO)[c]
M = Mn, R$_1$ = R$_2$ = H			
R = *i*-Pr	420 (420.1)	3278 (2439)	2034 (m), 1997 (vs), 1964 (s), 1939 (s), 1919 (m), 1907 (s)
R = c-Hex	500 (500.2)	3290	2032 (m), 1995 (vs), 1962 (s), 1938 (s), 1916 (m), 1904 (s)
R = *t*-Bu	448 (448.1)	3288 (2434)	2033 (m), 1995 (vs), 1963 (s), 1936 (s), 1918 (m), 1905 (m)
R = *p*-tol	(516.2)	3305	2034 (s), 1998 (vs), 1960 (s), 1934 (vs), 1920 (sh), (d)
M = Mn, R$_1$ = R$_2$ = CH$_3$, R = c-Pr	444 (444.1)	3278	2028 (s), 1988 (vs), 1949 (s), 1925 (s), 1908 (sh), (d)
M = Mn, R$_1$ = CH$_3$/H R$_2$ = H/CH$_3$			
R = *i*-Pr	434 (434.1)	3288	2031 (m), 1994 (vs), 1960 (s), 1936 (s), 1916 (m), 1903 (m)
M = Re, R$_1$ = R$_2$ = H			
R = *i*-Pr	552 (551.3)	3274	2030 (s), 1998 (vs), 1954 (s), 1921 (vs), 1902 (s), (d)
R = *t*-Bu	580 (579.4)	3278	2029 (s), 1998 (vs), 1953 (s), 1920 (vs), 1903 (s), (d)

[a] The observed M values account for the highest peak of the isotope pattern. [b] cm^{-1}, in KBr pellet (ν(ND)). [c] cm^{-1}; in hexane. [d] In dichloromethane.

conversion of the neutral *t*-Bu-DAB into the anionic *t*-Bu-AAA ligand indeed changes the character of the ligand completely (see Figure 3). In four- or eight-electron-bonded R-DAB complexes, the ligand is approximately flat, while in six-electron-bonded R-DAB complexes the ligand is almost flat with a maximum dihedral angle between the two imine bonds of 13°.[11]

According to the electronic bonding situation in the present compound, containing a formally monoanionic *t*-Bu-AAA ligand and a single Mn^0–Fe^I bond, each of the metals possesses a closed-valence shell.

IR Spectra: ν(CO) and ν(NH) Region. All [FeM(CO)$_6$(R–AAA)] complexes show characteristic absorption patterns in the ν(CO) region (see Table III). There are six CO stretching frequencies, all in the terminal region; i.e., between 2035 and 1900 cm^{-1}. The ν(CO) of the semibridging carbonyl cannot be distinguished from the ν(CO)'s of the terminal carbonyls. The spectra in solution (*n*-hexane or dichloromethane) are comparable to those obtained in a KBr disk, indicating that the structures in the solid state and in solution are similar.

The new N–H bond gives rise to an absorption in the ν(NH) region at ca. 3290 cm^{-1}. In the product obtained from the reaction of [Mn(CO)$_3$(R-DAB)Br] with [DFe(CO)$_4$]$^-$, this absorption is absent and a new signal is observed at ca. 2430 cm^{-1}. This can be assigned to the N–D stretching frequency on the basis of the calculated (harmonic) and measured ν(NH)/ν(ND) values (see Table IV).

FD-Mass Spectroscopy. In this study FD-mass spectroscopy has also been found to be an excellent method for the identification of the new products.[28] The presence of one Fe atom in the complexes is evidenced by the Fe isotope pattern of the parent ion (^{56}Fe 91.7, ^{54}Fe 5.8, and ^{57}Fe 2.2%) while the presence of one Re atom in [FeRe(CO)$_6$(R-AAA)] was also clearly indicated by the isotope pattern of its parent ion (^{187}Re 62.9 and ^{185}Re 37.1%). In Figure 4 the observed and calculated spectra for [FeMn(CO)$_6$(t-Bu-AAA)] are compared. All results are summarized in Table IV.

^{1}H NMR Spectroscopy. The ^{1}H NMR data are listed in Table V. When R-DAB is in a four-, six-, or eight-electron-coordination mode (see Figure 1), specific features

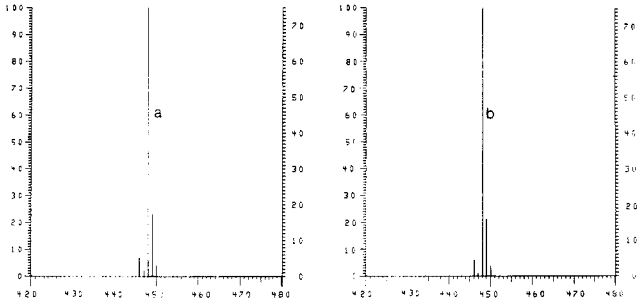

Figure 4. Observed (a) and calculated (b) mass spectra of [FeMn(CO)$_6$(*t*-Bu-AAA)].

of the ^{1}H NMR spectrum reveal what kind of coordination is present. In the symmetrical four- or eight-electron-bonding mode the imine protons give rise to one singlet at about 8 and 6 ppm, respectively, while in both cases the R groupings appear as one pattern. In the asymmetrical six-electron-bonding mode the imine protons give rise to an AX pattern at about 8 and 4 ppm (J = 2 Hz) while the two inequivalent R groupings resonate at two different chemical shift positions.[3,4b,11,14b]

Clearly none of these typical features are present in the ^{1}H NMR spectrum of [FeM(CO)$_6$(R-AAA)], and the conversion of the R-DAB ligand is directly evident. The amine proton on N(2) gives rise to a broad absorption at about 2.5 ppm. The allylic protons H(8) and H(7), bonded to C(8) and C(7), respectively (see Figure 2), occur at ±3.5 (virtual t, J = 2 Hz) and 6.7 ppm (d, J = 2 Hz). These resonance values may be compared with similar values found in the 3-amino-1-azaallylic derivative [Ru$_2$(CO)$_5${(*i*-Pr)N⋯CH⋯CHN(*i*-Pr)C(O)CH$_2$C(O)CH$_2$}], being 3.40 and 6.69 ppm, respectively.[25] Direct evidence for such a proton sequence in the ligand is obtained from saturation and deuteration experiments (vide infra).

When the broad signal at 2.5 ppm is irradiated, the remaining allylic protons occur as an AX pattern (see Figure 5). Irradiating H(8) results in a singlet pattern for H(7), while irradiating H(7) results in a doublet structure for H(8). In these cases the amine proton signal is hardly disturbed.

When [DFe(CO)$_4$]$^-$ is reacted with [Mn(CO)$_3$(R-DAB)Br] (R = *i*-Pr, *t*-Bu), [FeMn(CO)$_6${RNC(H)C(H)N(D)R}] is formed exclusively. The ^{1}H NMR spectrum of the

---

[28] (a) Mann, B. E. *Adv. Organomet. Chem.* **1974**, *12*, 135. (b) Jolly, P. W.; Mynott, R. *Adv. Organomet. Chem.* **1980**, *19*, 257.

Table V. ^{1}H NMR Data[a] for $[\mathrm{FeM(CO)_6(RN\overline{\cdot\cdot}C(R_1)\overline{\cdot\cdot}C(R_2)N(H)R)}]$

compd	R group[b]	NH	R_1	R_2
M = Mn, R_1 = R_2 = H				
R = *i*-Pr	3.97 (1 H; sept^e), 2.21 (1 H, sept^e), 1.84 (3 H, d^e)/1.63 (3 H, d^e), 0.94 (6 H, d^e)	2.14 (1 H, br)	6.69 (1 H, d^c)	3.40 (1 H, vt^c)
R = c-Hex	3.41 (1 H, m), 2.1–1.0 (21 H, m)	2.8 (1 H, br)	6.72 (1 H, d^c)	3.41 (1 H, m)
R = *t*-Bu	1.66 (9 H, s), 0.98 (9 H, s)	2.26 (1 H, br)	6.66 (1 H, d^c)	3.62 (1 H, vt^c)
R = *p*-tol^f	7.78 (2 H, d^g)/7.00 (2 H, d^g), 6.90 (2 H, d^g)/6.49 (2 H, d^g), 2.20 (3 H, s), 2.19 (3 H, s)	2.87 (1 H, br)	6.60 (1 H, d^c)	3.54 (1 H, m)
M = Mn, R_1 = R_2 = CH_3, R = c-Pr	1.3–0.3 (10 H, m)	1.67 (1 H, br)	2.71 (3 H, s)	1.63 (3 H, s)
M = Mn, R_1 = H, R_2 = CH_3, R = *i*-Pr^h	3.92 (1 H, sept^e), 2.91 (1 H, sept^e), 1.83 (3 H, d^e)/1.60 (3 H, d^e), 1.01 (3 H, d^e)/0.77 (3 H, d^e)	2.6 (1 H, br)	6.40 (1 H, s)	1.49 (3 H, s)
M = Mn, R_1 = CH_3, R_2 = H, R = *i*-Pr^h	4.21 (1 H, sept^e), 1.95 (1 H, sept^e), 1.72 (3 H, d^e)/1.50 (3 H, d^e), 0.95 (3 H, d^e)/0.93 (3 H, d^3)	1.95 (1 H, br)	2.57 (3 H, s)	3.55 (1 H, d^c)
M = Re, R_1 = R_2 = H				
R = *t*-Bu	1.60 (9 H, s), 1.05 (9 H, s),	3.02 (1 H, br)	7.33 (1 H, d^c)	3.89 (1 H, vt^c)
R = *i*-Pr	3.72 (1 H, sept^e), 2.48 (1 H, sept^e), 1.63 (3 H, d^e)/1.60 (3 H, d^e), 0.99 (3 H, d^e)/0.95 (3 H, d^e)	3.08 (1 H, br)	7.36 (1 H, d^c)	3.71 (1 H, vt^c)

[a] The values (ppm relative to Me_4Si) have been obtained in $CDCl_3$ solutions. [b] Vertical bars separate diastereotopic pairs; s = singlet, d = doublet, br = broad, m = multiplet, sept = septet, vt = virtual triplet. [c] J = 2 Hz. [e] J = 6 Hz. [f] In toluene-d_8 solution. [g] J = 8 Hz. [h] These two isomers could not be separated, and the ^{1}H NMR spectrum of mixture was recorded.

Table VI. ^{13}C NMR Data for $[\mathrm{FeM(CO)_6(RN\overline{\cdot\cdot}C(R_1)\overline{\cdot\cdot}C(R_2)N(H)R)}]$

compd	R and $C(R_2)$[b]	CO	$C(R_1)$
M = Mn, R_1 = R_2 = H			
R = *i*-Pr	67.7, 64.8, 58.0 (N–$C^{i\text{-Pr}}$ and $C(R_2)$), 29.5/24.3, 21.3/19.7 (CH_3)	226.0 (br)^c 217.8	101.1
R = c-Hex	73.5, 66.7 (N–$C^{c\text{-Hex}}$ and $C(R_2)$), 41.8, 37.0, 31.9, 30.9, 27.3, 27.0, 26.5, 25.9 (C^{ring})	226.7 (br) 217.8	102.2
R = *t*-Bu	64.5, 59.0 (N-$C^{t\text{-Bu}}$), 64.3 ($C(R_2)$)	225.6 (br) 217.8	105.1
M = Mn, R_1 = R_2 = CH_3, R = c-Pr	82.2 ($C(R_2)$), 44.1, 41.1, (N-$C^{c\text{-Pr}}$), 21.7, 18.1 (CH_3), 11.9/10.8, 9.9/4.1 (C^{ring})	215.9	117.4

[a] The values (ppm relative to Me_4Si) have been obtained in $CDCl_3$ solutions at 30 °C. [b] Vertical bars separate diastereotopic pairs; br = broad. [c] At −60 °C, this peak splits into three sharp signals: 227.4, 227.0, and 220.5 ppm. [d] At −60 °C, this peak splits into three sharp signals: 227.7, 227.0, and 221.2 ppm.

deuterated compound lacks the N–H signal, and the remaining allylic hydrogens are observed as an AX pattern.

Finally the very different chemical shift positions of the two R groupings is in line with the conversion of the R-DAB ligand into the highly asymmetric R-AAA ligand.

When $[HFe(CO)_4]^-$ is reacted with $[Mn(CO)_3(i\text{-Pr-DAB}\{H,Me\})Br]$, one can expect two possible isomeric products: one with the Me group bonded to C(7) and one with the Me group on C(8). The ^{1}H NMR spectrum of the reaction mixture shows that indeed both isomers are formed in a ratio of about 1:2. The two isomers could not be separated, and further experiments at different reaction temperatures did not influence the product ratio. The ^{1}H NMR data of both isomers are included in Table V and are in accord with the assignment for the allylic protons given above.

^{13}C NMR Spectroscopy. The ^{13}C NMR data of the $[FeMn(CO)_6(R\text{-AAA}\{R_1,R_2\})]$ compounds are listed in Table VI and are in accord with the molecular geometry in solution that is similar to that found for M = Mn, R = *t*-Bu, and R_1 = R_2 = H in the solid state. C(7) and C(8) (see Figure 2) are observed in the allylic region[28] at about 100 and 70 ppm, respectively. In two other azaallylic compounds, $[Ru_2(CO)_5\{(i\text{-Pr})\overline{NC(H)C}(H)N(i\text{-Pr})C(O)CH_2C(O)CH_2\}]$[25] and $[Fe_2(CO)_6\{(C_{10}H_{11})\overline{NC(CO_2Me)C}(CO_2Me)\}]$,[24] these values are 104 and 57 ppm and 125.8 and 112.0 ppm, respectively. The higher values found for the latter compound can be explained by the presence on the allylic carbons of strongly electron-withdrawing substituents. The two inequivalent R groups give rise to two different chemical shift patterns.

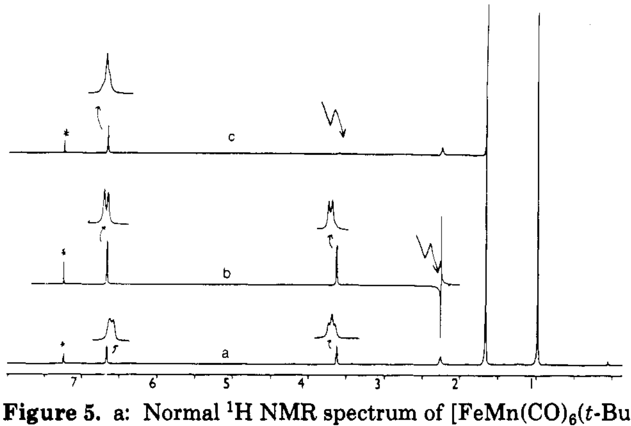

Figure 5. a: Normal ^{1}H NMR spectrum of $[FeMn(CO)_6(t\text{-Bu-AAA})]$. b: Irradiated at N–H (2.3 ppm). c: Irradiated at C(8)–H(8) (3.6 ppm) (the asterisk is $CHCl_3$).

The six carbonyl groups have resonances at 226 (br) and 217 ppm, at +30 °C. Lowering the temperature to −40 °C does not influence the signal at 217 ppm, but the signal

Table VII. Elemental Analyses[a] for [$FeM(CO)_6$(R-AAA{R_1,R_2})]

compd	mol formula	mass	%C	%H	%N
M = Mn, R_1 = R_2 = H					
R = *i*-Pr	$FeMnC_{14}H_{17}N_2O_6$	420.1	39.94 (40.03)	4.03 (4.08)	6.64 (6.67)
R = c-Hex	$FeMnC_{20}H_{25}N_2O_6$	500.2	48.10 (48.02)	5.20 (5.04)	5.54 (5.60)
R = *t*-Bu[b]	$FeMnC_{16}H_{21}N_2O_6$	448.1	42.95 (42.88)	4.79 (4.72)	6.20 (6.25)
M = Mn, R_1 = R_2 = CH_3, R = c-Pr	$FeMnC_{16}H_{17}N_2O_6$	444.1	43.20 (43.27)	3.72 (3.86)	6.13 (6.31)
M = Re, R_1 = R_2 = H					
R = *i*-Pr	$FeReC_{14}H_{17}N_2O_6$	551.3	30.44 (30.49)	3.11 (3.11)	4.90 (5.08)
R = *t*-Bu	$FeReC_{16}H_{21}N_2O_6$	579.4	33.13 (33.16)	3.73 (3.66)	4.74 (4.84)

[a] Found (calcd). [b] Fe, 12.56 (12.46).

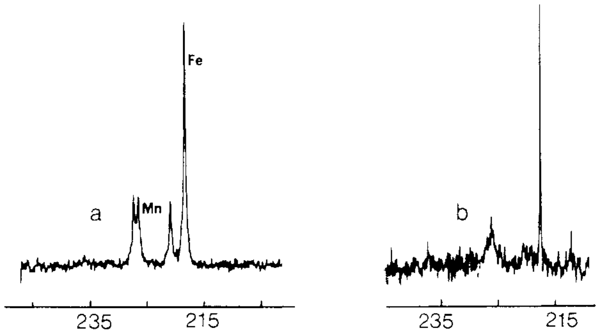

Figure 6. Carbonyl region of the ^{13}C NMR spectrum of [$FeMn(CO)_6$(*i*-Pr-AAA)] at -60 C (a) and at +20 °C (b).

at 226 ppm is replaced by three sharp signals (see Figure 6). According to the literature,[28-30] the peak at 217 ppm may be assigned to the three rapidly scrambling carbonyl groups on Fe (including the semibridging one), while the three carbonyl groups on Mn give rise to three signals at low temperature (slow exchange). The ^{13}C NMR spectra of the present compounds in the carbonyl region at low temperature and those of reported[30] [$CoMn(CO)_6$(R-DAB)] complexes are very much alike. The three carbonyl groups bonded to Co (including a semibridging one) in the latter complexes give rise to one signal, while the three carbonyl groups bonded to Mn give rise to three separate signals.

Other Reactions. Interestingly, [$Fe(CO)_4$]$^{2-}$ reacts with [$Mn(CO)_3$(R-DAB)Br] (R = *i*-Pr, *t*-Bu) to give similar [$FeMn(CO)_6$(R-AAA)] products. In that case the amine proton is most probably obtained by H abstraction from the THF solvent.[31]

When the [$HFe(CO)_4$]$^-$ anion was isolated with the $(Ph_3P)_2N$ cation, it reacted not at all (M = Re) or only very slowly (M = Mn) with [$M(CO)_3$(R-DAB)Br]. This is in accord with earlier findings reported in the literature that this tight cation–anion pair has a lower reactivity than the alkali-metal salts.[32]

Discussion

Reaction Route. At present the precise reaction route leading to the formation of the heterodimetallic 3-amino-1-azaallylic products is not certain though a chemically reasonable reaction path is given in Scheme I.

In the first step Br^- is replaced by [$HFe(CO)_4$]$^-$. A similar substitution is found in the reaction of [$Co(CO)_4$]$^-$ with [$M(CO)_3$(R-DAB)Br] (M = Mn, Re).[11] The first step, yielding intermediate A, is then followed by intramolecular rearrangements, involving an insertion of one C=N double bond into the Fe—H bond, after which CO elimination and coordination of the second C=N double bond yield the final product. Double-bond insertion into the Fe–H bond of [$HFe(CO)_4$]$^-$ has been suggested as a first step in the hydrogenation or reduction reactions of olefins with [$HFe(CO)_4$]$^-$.[33] In one instance such an organoiron intermediate, i.e., [$(PPh_3)_2N$][$(CO)_4Fe${C(H)(Me)COOMe}], was claimed to be isolated.[33a]

Scheme I

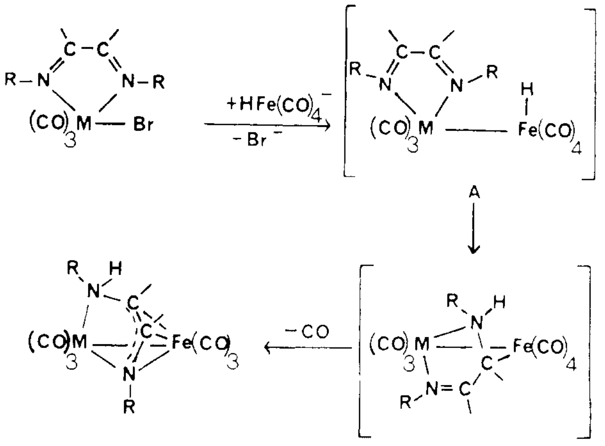

Scheme II

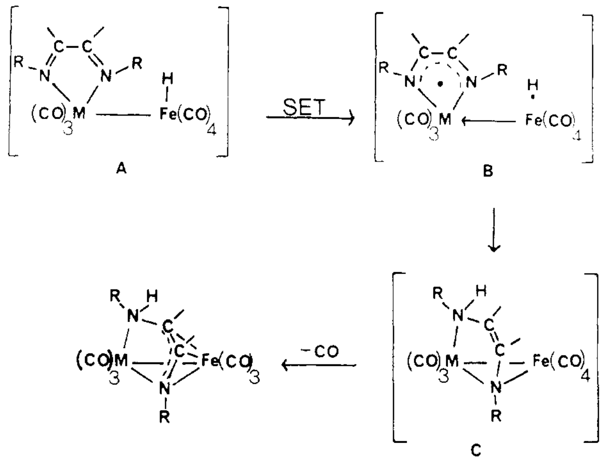

A mechanism that differs from the one outlined in Scheme I with respect to the rearrangements taken place in intermediate A involves a single electron transfer (SET) and is depicted in Scheme II.

After the formation of intermediate A, a SET step takes place, which results in a radical pair containing a [M-

---

(29) Todd, L. J.; Wilkinson, J. R. *J. Organomet. Chem.* **1974**, *77*, 1.

(30) Staal, L. H.; Keijsper, J.; Polm, L. H.; Vrieze, K. *J. Organomet. Chem.* **1981**, *204*, 101 and references therein.

(31) Cf. Takegami, Y.; Watanabe, Y.; Mitsudo, T.; Okajima, T. *Bull. Chem. Soc. Jpn.* **1969**, *42*, 1992.

(32) (a) Collman, J. P. *Acc. Chem. Res.* **1975**, *8*, 342. See also ref 16. (b) Darensbourg, M.; Borman, C. *Inorg. Chem.* **1976**, *15*, 3121.

(33) (a) Mitsudo, T.; Watanabe, J.; Yamashita, M.; Takegami, Y. *Chem. Lett.* **1974**, 1385. (b) Mitsudo, T.; Watanabe, J.; Nakaniski, H.; Morishima, I.; Inubushi, T.; Takegami, Y. *J. Chem. Soc., Dalton Trans.* **1978**, 1298. (c) Yamashita, M.; Miyoshi, K.; Okada, Y.; Suemitsu, R. *Bull. Chem. Soc. Jpn.* **1982**, *55*, 1329.

(CO)$_3$(R-DAB)]· radical part. The existence of this type of radical (M = Mn) has been proven in 2-MeTHF, at 230 K, with the ESR technique (a_{Mn} = 9.53, a_{N} = 7.40, and a_{H} = 4.75 G).[34] Migration of the H atom, within the radical pair, will then result in N–H bond formation because in the [M(CO)$_3$(R-DAB)]· radical part the spin density on the N atoms is expected to be higher than that on the imine C atoms.[35] An indication for the presence of a SET mechanism may be the reaction of [M(CO)$_3$(*p*-tol-DAB)-Br][17b] with an excess of [HFe(CO)$_4$]$^-$ which yields primarily [HFeMn{N(*p*-tol)CH$_2$CH$_2$N(*p*-tol)}]. During this reaction two new C(ligand)–H bonds are formed. In a [M(CO)$_3$-(*p*-tol-DAB)]· radical part, belonging to a radical pair analogous to B shown in Scheme II, the spin density on the N atoms will be delocalized over the aryl rings, making N–H bond formation kinetically less favorable than C–H bond formation. During the final step (scheme II), which is analogous to that shown in Scheme I, η^2-coordination of the double bond and loss of CO yield the 3-amino-1-azaallylic product.

Another possible progression following the substitution step may be a H$^-$ transfer from the Fe hydride reagent to the ligand skeleton. Due to the difference in electronegativity between the imine C and N atoms, one may anticipate that the H atom ends up on the C atom. However, α,β-unsaturated compounds often give addition reactions analogous to the well-documented Michael addition.[36] If the present reactions proceed via a Michael addition-like step, the same intermediate C, as shown in Scheme II, will be present.

In all mechanisms discussed, CO elimination takes place after proton migration from iron to the ligand. This is in line with the observation that [FeRe(CO)$_6$(*i*-Pr-AAA)] reacts when heated to yield the isomeric hydride [HFeRe(CO)$_6$(*i*-Pr-DAB)].[17a] During this reaction the *i*-Pr-AAA ligand is converted back to the neutral *i*-Pr-DAB ligand, by migration of the amine proton to the metal core. The resulting hydride does not react further, indicating that it is thermodynamically more stable than the 3-amino-1-azaallylic derivative.

The hydride iron anion [HFe(CO)$_4$]$^-$ has been used as a desulfurization agent[37] and as an effective carbonylation, reduction, hydrogenation, hydroacylation, and reductive alkylation agent toward a large variety of functional groups.[33,38] In many cases an (η^3-allyl)Fe intermediate has been proposed[31,33b,c] but, to our knowledge, never been isolated. With [FeM(CO)$_6$(R-AAA)] (M = Mn, Re), we have obtained a species, having such an η^3-allyl arrangement, in which one C=N double bond is partly reduced by the iron hydride reagent, that places the earlier intermediate proposals on a more definite basis.

Conclusions

Neutral R-DAB can be reduced to the monoanionic 3-amino-1-azaallylic grouping as a result of hydride migration from a metal center.

Coordinated R-DAB may be activated at the imine N atom that can lead to N–H bond formation; in homodinuclear [Ru$_2$(CO)$_n$(R-DAB)] (n = 5, 6) activation is found primarily at the imine C atom.

The η^3-allylic arrangement can be considered as a model for the intermediate stage during the reaction of propenylic bonds by [HFe(CO)$_4$]$^-$.

Acknowledgment. We thank D. Heijdenrijk for collecting the X-ray data, R. Fokkens for recording the mass spectra, and J. M. Ernsting for recording the 250-MHz NMR spectra. We thank the Netherland Foundation for chemical research (SON) and the Netherland Organization for pure research (ZWO) for their financial support.

Registry No. [FeMn(CO)$_6$(*t*-Bu-AAA)], 91443-19-5; [FeMn-(CO)$_6${(*t*-Bu)$\overline{\mathrm{NC(H)C}}$(H)N(D)(*t*-Bu)}], 91466-40-9; [FeMn(CO)$_6$-(*i*-Pr-AAA)], 91443-20-8; [FeMn(CO)$_6${(*i*-Pr)$\overline{\mathrm{NC(H)C}}$(H)N(D)(*i*-Pr)}], 91443-21-9; [FeMn(CO)$_6$(c-Hex-AAA)], 91443-22-0; [FeMn(CO)$_6$(*p*-tol-AAA)], 91443-23-1; [FeMn(CO)$_6$(c-Pr-AAA-{CH$_3$,CH$_3$})], 91443-24-2; [FeMn(CO)$_6$(*i*-Pr-AAA{CH$_3$,H})], 91443-25-3; [FeMn(CO)$_6$(*i*-Pr-AAA{H,CH$_3$})], 91443-26-4; [FeRe(CO)$_6$(*i*-Pr-AAA)], 91443-27-5; [FeRe(CO)$_6$(*t*-Bu-AAA)], 91443-28-6; [Mn(CO)$_3$(*i*-Pr-DAB)Br], 70773-65-8; [Mn(CO)$_3$(c-Hex-DAB)Br], 64538-57-4; [Mn(CO)$_3$(*t*-Bu-DAB)Br], 70749-13-2; [Mn(CO)$_3$(*p*-tol-DAB)Br], 70708-87-1; [Mn(CO)$_3$(*i*-Pr-DAB-{CH$_3$,H})Br], 75548-76-4; [Mn(CO)$_3$(c-Pr-DAB{CH$_3$,CH$_3$})Br], 75548-77-5; [Re(CO)$_3$(*i*-Pr-DAB)Br], 75548-79-7; [Re(CO)$_3$(*t*-Bu-DAB)Br], 70708-92-8; Na[HFe(CO)$_4$], 53558-55-7; Na[DFe-(CO)$_4$], 91443-29-7; Fe(CO)$_5$, 13463-40-6.

Supplementary Material Available: Tables of observed and calculated structure factors, the final anisotropic thermal parameters, and all bond angles (30 pages). Order information is given on any current masthead page.

---

(34) Kokkes, M. W.; Stufkens, D. J.; Oskam, A., to be submitted for publication.

(35) In the reaction of Et$_2$Zn with *t*-Bu-DAB, Et$_2$Zn(*t*-Bu-DAB) is formed in a first step. Warming up the reaction mixture yielded only a N-ethylated product. This was explained by a mechanism involving a single electron transfer, yielding a {[EtZn(*t*-Bu-DAB)]·Et·} radical pair. ESR data obtained from the [EtZn(*t*-Bu-DAB)]· radical, indicated a greater spin density on the imine N atom (0.3) than on the imine C atom (0.2). van Koten, G.; Jastrzebski, J. T. B. H.; Vrieze, K. *J. Organomet. Chem.* **1983**, *250*, 49.

(36) Kashima, C.; Aoki, Y.; Omote, Y. *J. Chem. Soc., Perkin Trans.* **1975**, *2511*.

(37) Alper, H.; Paik, H. N. *J. Org. Chem.* **1977**, *42*, 3522.

(38) (a) Watanabe, Y.; Shim, S. C.; Mitsudo, T.; Yamashita, M.; Takegami, Y. *Bull. Chem. Soc. Jpn.* **1976**, *49*, 1378 and references therein. (b) Watanabe, Y.; Takasuki, K.; Shim, S. C.; Mitsudo, T.; Takegami, Y. *Ibid.* **1978**, *51*, 3397. (c) Watanabe, Y.; Sim, S. C.; Mitsudo, T.; Yamashita, M.; Takegami, Y. *Ibid.* **1978**, *49*, 2302. (d) Watanabe, Y.; Shim, S. C.; Uchida, H.; Mitsudo, T.; Takegami, Y. *Tetrahedron* **1979**, *35*, 1433. (e) Cainelli, G.; Panunzio, M.; Umani-Rouchi, A. *J. Chem. Soc., Perkin Trans. 1* **1975**, 1273. (f) Marko, L.; Radhi, M. A.; Otvös, I. *J. Organomet. Chem.* **1981**, *218*, 369. (g) Cole, T. E.; Pettit, R. *Tetrahedron Lett.* **1977**, 781. (h) Boldrini, G. P.; Umani-Rouchi, A.; Panunzio, M. *Synthesis* **1976**, *9*, 596 and references therein.